EAI Endorsed Transactions
on Internet of Things
Research Article EAI.EU

Performance Evaluation of Various Path Planning Methods for Robotics and Computational Geometry

Gokuldas Vedant Sarvesh Raikar[1], Gururaj H. L[2], Vinayakumar Ravi[3,*], Wael Suliman[3]

[1]Department of Computer Science and Engineering, Manipal Institute of Technology Bengaluru, Manipal Academy of Higher Education, Manipal 560064, India

[2]Department of Information Technology, Manipal Institute of Technology, Manipal Academy of Higher Education, Bengaluru 560064, India

[3]Center for Artificial Intelligence, Prince Mohammad Bin Fahd University, Khobar, Saudi Arabia

Abstract

INTRODUCTION: In integrating Spiral Coverage into Cellular Decomposition, which combines structured grid-based techniques with flexible, quick spiral traversal, time efficiency is increased.
OBJECTIVES: In the field of robotics and computational geometry, the study proposes a comparative exploration of two prominent path planning methodologies—Boustrophedon Cellular Decomposition and the innovative Spiral Coverage. Boustrophedon coverage has limitations in time efficiency due to its back-and-forth motion pattern, which can lead to lengthier coverage periods, especially in congested areas. Nevertheless, it is useful in some situations. It is critical to address these time-related issues to make Boustrophedon algorithms more useful in practical settings.
METHODS: The research centres on achieving comprehensive cell coverage, addressing the complexities arising from confined spaces and intricate geometries. While conventional methods emphasise route optimization between points, the coverage path planning approach seeks optimal paths that maximize coverage and minimize associated costs. This study delves into the theory, practical implementation, and application of Spiral Coverage integrated with established cellular decomposition techniques.
RESULTS: Through comparative analysis, it illustrates the advantages of spiral coverage over boustrophedon coverage in diverse robotics and computational applications. The research highlights Spiral Coverage's superiority in terms of path optimization, computational efficiency, and adaptability, proposing a novel perspective into cell decomposition. The methodology integrates the Spiral Coverage concept, transcending traditional techniques reliant on grids or Voronoi diagrams. Rigorous evaluation validates its potential to enhance path planning, exemplifying a substantial advancement in robotics and computational geometry.
CONCLUSION: Our findings show that spiral coverage is on an average 45% more efficient than conventional Boustrophedon coverage. This paper set the basis for the future work on how different algorithms can traverse different shapes more efficiently.

Keywords: Path planning, Computational geometry, Boustrophedon Cellular Decomposition, Spiral Coverage, Coverage Path Planning.

Received on 15 03 2024, accepted on 31 10 2024, published on 12 11 2024

doi: 10.4108/eetiot.5433

*Corresponding author. Email: vravi@pmu.edu.sa

1. Introduction

Coverage path planning (CPP) presents the challenge of determining optimal pathways for robots to traverse entire environments, a departure from traditional point-to-point navigation. Practical applications like floor cleaning [1], grass mowing [2], mine hunting [3], and harvesting [4] require thorough coverage. Unlike point-to-point planning, CPP aims to maximize coverage while minimizing parameters like time to completion. Early methods involved behaviour-based approaches with heuristic and random elements [5,6]. Modern CPP algorithms often use cellular decomposition to achieve complete coverage by dividing the target region into cells, ensuring coverage within each cell [5,6]. This approach is crucial in applications such as agriculture and cleaning robotics, optimizing routes for efficient coverage, resulting in time and resource savings, and enhancing the operational efficiency of autonomous systems. Enric Galceran's classification [7] identifies Morse-based cellular decomposition, encompassing On-line Morse-based boustrophedon and Morse-based with Voronoi, and classical cellular decomposition with Trapezoidal and Boustrophedon subcategories. Trapezoidal decomposition achieves thorough coverage in planar spaces, while the "classical" boustrophedon decomposition generates shorter paths for complete coverage. Morse-based cellular decomposition is advantageous in environments with differentiable barrier borders, utilizing range sensor data to identify crucial cell boundaries [7].

Spiral coverage, characterized by continuous movement in a spiral pattern, offers a promising path planning strategy in robotics and computational applications, providing adaptability to uneven terrains, efficient area coverage, and shorter path lengths. In contrast, Boustrophedon path planning involves systematic back-and-forth movements, suitable for comprehensive coverage in applications like environmental monitoring and agriculture. This work introduces a revolutionary approach by integrating Spiral Coverage into Cellular Decomposition, combining spiral traversal and structured grid-based methods to significantly enhance path planning efficiency. Critiquing the limitations of Boustrophedon Cellular Decomposition, the study advocates for comprehensive cell coverage with optimized paths to maximize coverage while minimizing costs, demonstrating the superiority of Spiral Coverage, which proves to be, on average, 45% more efficient than traditional Boustrophedon coverage [1]. This advancement contributes to algorithm development for effective traversal across various shapes, pushing the boundaries of computational geometry and robotics.

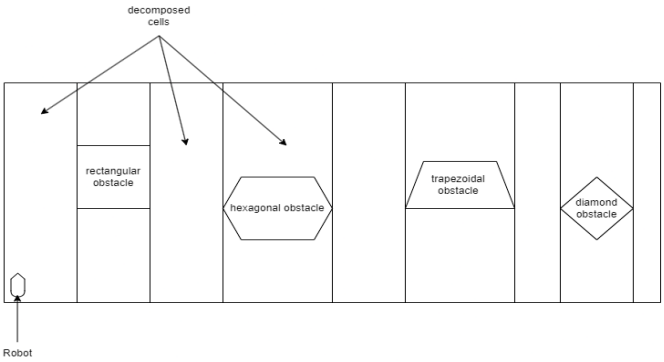

Figure 1. Represents the environment, which is decomposed into cells, it also contains a robot which will the cover the decomposed cells using different algorithm. Here the rectangular, hexagonal, trapezoidal, diamond shape represents the obstacles. The robot represented on the left lower corner is used to traverse decomposed cells either using boustrophedon or spiral coverage.

Our study aims to enhance path optimization, computational efficiency, and adaptability across various robotics and computational applications. We propose a ground-breaking integration of spiral coverage with the well-established Boustrophedon approach to minimize travel times, reduce energy consumption, and improve overall path planning efficiency. Unlike conventional grid-based methods, our approach demonstrates adaptability to uneven terrains and congested environments. Departing from traditional grid and Voronoi diagram techniques, we offer a fresh perspective on cell decomposition. The versatility of our approach is evidenced by its application in real-world scenarios, including autonomous robotics, precision farming, surveillance, and search and rescue. Through in-depth comparative analysis, we highlight the distinct advantages of our proposed technique and project its potential to revolutionize the fields of robotics and computation, aiming to provide a comprehensive and innovative path planning approach surpassing current strategies' limitations.

In Figure 2, a robot is depicted with three ultrasonic sensors strategically positioned to detect obstacles in front, left, and right directions. These sensors emit ultrasonic waves, measuring distances by analyzing echoes, enabling the robot to navigate safely through dynamic environments by altering its course or halting to prevent collisions. The paper is organized into six sections, starting with an introduction (Section 1) that establishes the context for the comparative study of Boustrophedon cellular decomposition and spiral coverage in robotics and computational geometry. This section underscores the significance of these methods in the field.

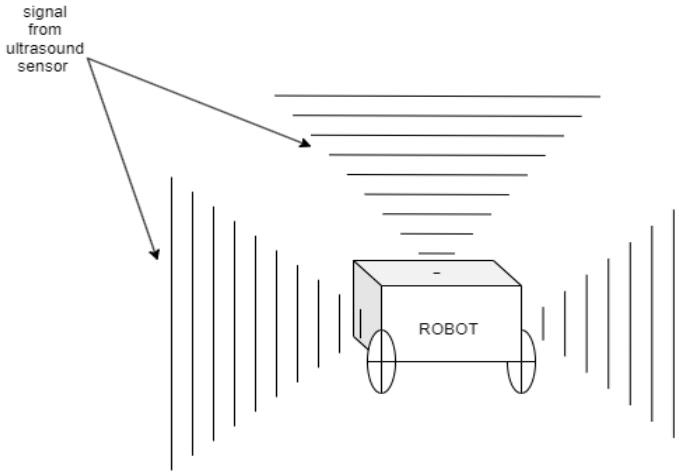

Figure 2. Depicts the robot which has three ultrasound sensors to sense the obstacles in the three directions. These three sensors are used to sense the obstacles in the forward, left and right direction if all these sensors are high the move in the backward direction.

The paper is organized as follows; Section 2 conducts a thorough review of existing literature, exploring the strengths and weaknesses of both Boustrophedon cellular decomposition and spiral coverage while identifying areas for further investigation. Sections 3 and 4 delve into the experimental setup, providing detailed information on methodology and simulation analysis. These sections contribute a comprehensive review of the comparative study's results. The concluding Section 5 synthesizes key findings and outlines potential avenues for future research, discussing the prospects and potential advancements in Boustrophedon cellular decomposition and spiral coverage in robotics and computational geometry, thereby framing the paper's structure.

2. Literature Survey

In recent years, the field of robotics has witnessed notable progress, particularly in the domain of path planning, a crucial aspect of autonomous robot operations. This literature overview lays the foundation for a comparative investigation into Boustrophedon cellular decomposition and spiral coverage for optimizing cell coverage in robotics and computational geometry. Cai et al. [9] proposed a coverage path planning method for cleaning robots, employing the heuristic Ax in a U-turn search strategy to ensure efficient coverage and minimal repetition. Song and Gupta [10] introduced the εx algorithm for online coverage path design, utilizing an Exploratory Turing Machine and Multiscale Adaptive Potential Surfaces to achieve computational efficiency and total coverage. Bochkarev and Smith [11] explored sweep coverage path planning, optimizing turn count by estimating the minimum altitude of non-convex polygonal regions. Choset's boustrophedon cellular breakdown method [12] addressed coverage path planning challenges by segmenting environments into efficiently covered cells using back-and-forth motions, showcasing effectiveness in applications like de-mining and floor washing.

Brown and Waslander [22] demonstrate that while spiral coverage achieves complete coverage, it does not explicitly emphasize its efficiency in terms of time, leading to the foundation for this paper. In contrast, the Constriction Decomposition Method (CDM) provides a precise cellular decomposition technique for 2D coverage path planning, showcased in a complex indoor office environment [22]. Another study introduces a collaborative complete coverage path planning (CCPP) algorithm, optimizing incremental coverage for multi-robot systems [23]. Balampanis et al. propose a novel discretization method using Constrained Delaunay Triangulation for area decomposition, contributing to optimal path planning graph creation [24]. Energy-efficient coverage path planning for autonomous vehicles is explored by C. Wu et al., incorporating Fermat spiral paths and energy efficiency heuristics [25]. Yang et al. address nonrepetitive coverage paths for manipulators, utilizing finite cellular decomposition to minimize discontinuities [26]. Barrientos et al. describe a precision agriculture system using unmanned aerial vehicles [27]. This literature survey underscores the diverse applications and advancements in robotics path planning, spanning cleaning robots, precision agriculture, and manipulator coverage paths. Despite progress, challenges persist, prompting ongoing research into novel computational techniques, reinforcement learning, and geometric algorithms to address real-world complexities and enhance efficiency. Following a thorough analysis of the literature on boustrophedon coverage algorithms for robotics and autonomous systems, it is evident that while they have proven successful in some situations, they frequently fall short when faced with real-world difficulties. Increased travel distances, frequent, time-consuming twists, and the inability to adjust to varied obstacle densities and shapes are some of these difficulties, highlighting the urgent need for additional study to resolve these restrictions and improve boustrophedon coverage for more extensive and intricate operational contexts.

3. Methodology

Cellular decomposition, a well-established technique with profound implications in robotics and autonomous navigation, serves as the bedrock for partitioning intricate regions into discrete cells, thereby laying the foundation for efficient path planning. This technique has challenges when confronted by scenarios characterized by confined spaces, diverse barrier dimensions, and intricate geometries. Enter the revolutionary strategy of spiral coverage, poised to transcend these challenges, and revolutionize aspects of

path quality, adaptability, traversal efficiency, and the temporal requirements for achieving complete coverage.

This section presents a comprehensive methodology designed to seamlessly integrate the innovative concept of "spiral coverage" into cellular decomposition algorithms. The primary objective of this study is to significantly enhance the efficacy of path planning strategies, particularly in complex and cluttered environments and establishment of a systematic framework that not only applies the concept of spiral coverage but also rigorously evaluates its methodology. The research encompasses a set of pivotal goals, each contributing to the comprehensive integration of spiral coverage into existing cellular decomposition methodologies. For a visual representation of the suggested process, the text refers to Figure 3, a flow chart.

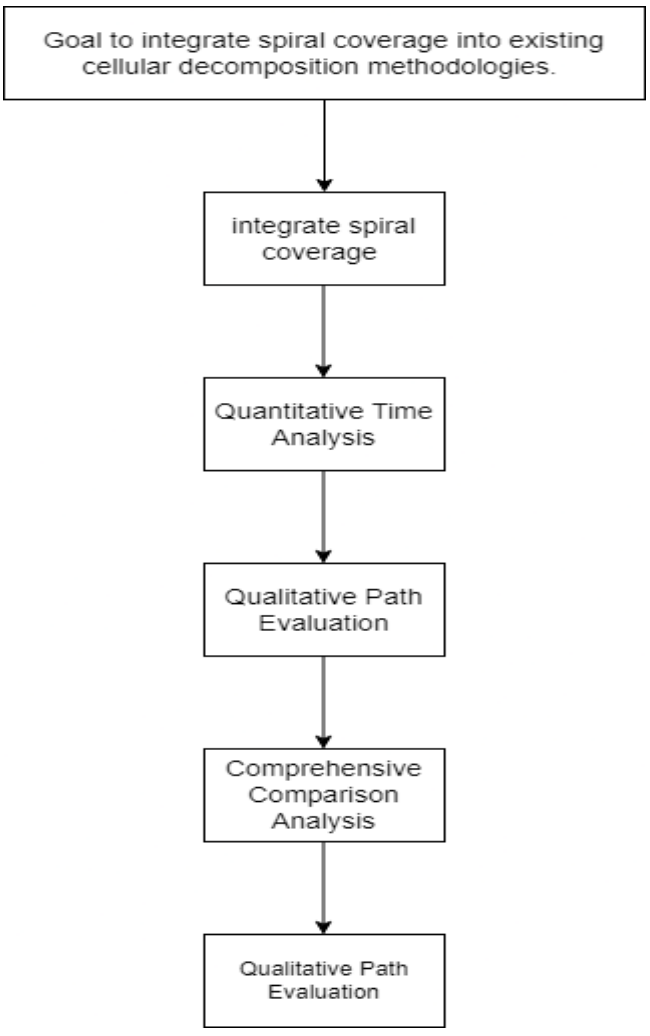

Figure 3. Flow chart depiction of integration of spiral coverage into existing cellular decomposition methodologies. Here are the steps a. integrate spiral coverage into existing cellular b. quantitative time analysis c. qualitative path evaluation d. comparison analysis.

3.1. Boustrophedon Cellular Decomposition

The boustrophedon cellular breakdown approach in robotics and autonomous navigation is depicted in Figure 4, which is described in the text. Robotics and autonomous navigation use the fundamental path planning method known as boustrophedon cellular decomposition, often known as zigzag decomposition. With this technique, a workspace or environment is divided into a few connected cells that are each traversed in a "zigzag" pattern and partition intricate spatial domains into discrete and well-defined zones, facilitating expeditious exploration for the purpose of ascertaining optimal pathways for robotic navigation. By systematically breaking down complex regions, the approach enables efficient analysis to identify the most suitable route for the robot's traversal. This method offers inherent simplicity and user-friendliness, rendering it an asset for addressing uncomplicated path planning necessities. Leveraging its deterministic characteristics, the solutions it yields are both foreseeable and reproducible, thereby amplifying its utility across diverse applications. The Boustrophedon decomposition excels in contexts necessitating meticulous coverage, such as cleaning or monitoring tasks, due to its methodical exploration of each cell through alternating traversal.

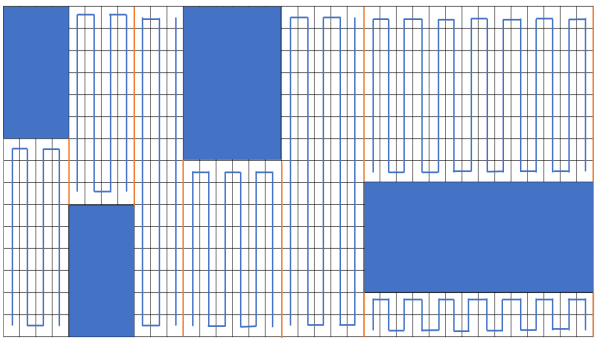

Figure 4. depicting the boustrophedon cellular decomposition. Each of the blue region in this figure represents the obstacle and the blue lines shows the path followed by the robot for the boustrophedon coverage of each decomposed cell.

In congested and complicated surroundings might result in inefficient pathways, prolonged trip times, or even navigation failures due to the slowness of boustrophedon decomposition. The performance of the stiff zigzag pattern may be hindered by its inability to adjust to complex geometries, constrained spaces, or irregularly shaped obstructions. The boustrophedon decomposition does not always result in paths with the shortest lengths or with the lowest energy consumption, which makes it less ideal than more sophisticated path planning techniques. Therefore, even though Boustrophedon Cellular Decomposition has advantages, it might not always be the best option in complex or dynamic path planning scenarios where

effectiveness and adaptability are crucial. The Cellular decomposition process begins with the supplied workspace, denoted as *P*, being subjected to polygonal decomposition, often achieved through methods like convex decomposition, resulting in the segmentation of the space into smaller polygons. Subsequently, the perimeter or boundary of each derived polygon is calculated to establish the delineation of the cells. Within each cell, a meticulous traversal path is delineated, frequently adopting a back-and-forth zigzag pattern to ensure comprehensive coverage. A critical facet of this decomposition is the establishment of a continuous path connecting the edges of adjacent cells, ensuring smooth path continuity. Optimization of the robot's movement both within and between cells, techniques such as the Traveling Salesman Problem (TSP) or Minimum Spanning Tree (MST) might be employed, depending on the specific application. Cellular decomposition can be represented as follows:

3.1.1 Algorithm: Polygon Decomposition and Traversal Planning

Start
Input:
- Polygon P with vertices V
- Grid dimensions Ni rows and Mi columns
- Subcell sizes wij and hij
- Connectivity points Tij for adjacent cells
- Objective function f(x) and constraints

Output:
- Traversal path for efficient coverage

1. DecomposePolygon(P, V):
- For each cell Ci in P:
- Calculate convex hull Ci = conv(Vi1, Vi2, ..., Vir, Vi1)

2. GenerateTraversalPath():
- For each cell Ci:
- Divide Ci into an Ni x Mi grid of subcells
- Traverse subcells to create a sequence of indices (r1, c1), (r2, c2), ..., (rp, cp)

3. EnsureCellConnectivity():
- For each adjacent cell pair Ci and Cj:
- Define transition points Tij and Tji that connect boundaries
- Ensure direct travel between Tij and Tji is possible

4. OptimizationProblem():
- Formulate an optimization problem:
- Objective function: min f(x) subject to constraints
- Decision variables x include subcell traversal order and transition points

5. SolveOptimizationProblem():
- Utilize mathematical programming techniques to solve the optimization problem

6. OutputResults():
- Obtain the optimized traversal path from the solution

Main:
- Call DecomposePolygon(P, V)
- Call GenerateTraversalPath()
- Call EnsureCellConnectivity()
- Call OptimizationProblem()
- Call SolveOptimizationProblem()
- Call OutputResults()

End

3.1.2 Explanation of Algorithm for Polygon Decomposition and Traversal Planning

An input parameter set for the "Polygon Decomposition and Traversal Planning" algorithm includes a polygonal workspace represented by its vertices (P with vertices V), the size of a grid for sub cell decomposition (Ni rows and Mi columns), the sub cell sizes (wij and hij), the connectivity points for adjacent cells (Tij), and an objective function (f(x)) with associated constraints. Planning a fast traversal path across the polygonal workspace is its main objective. The algorithm divides the complicated polygonal workspace (P) into simpler convex cells in the first phase, calculating the convex hull of each cell as it iterates through the polygon's cells (Ci).The traversal path is then generated for each convex cell (Ci) by splitting the cell into a Ni x Mi grid of sub cells and designing the traversal path within each cell. The algorithm provides connectivity between adjacent cells by establishing transition points (Tij and Tji) on their boundaries in order to guarantee continuous coverage across the full workspace. It then formulates an optimization problem to maximize traversal efficiency while taking into account specified restrictions, incorporating an objective function (f(x)) and decision variables (x). In order to address the optimization problem, the system finally uses mathematical programming techniques. It finds the optimal traversal path that optimally covers the polygonal workspace while respecting connection and other restrictions. This all-encompassing strategy provides a disciplined and flexible answer for coverage planning in a variety of settings.

3.2 Spiral Coverage

The introduction of the groundbreaking concept of "spiral coverage" is a major advancement in cellular decomposition for path planning, diverging from traditional methodologies and offering solutions to long-standing challenges. This innovative approach entails a systematic traversal method within each cell, guiding robots along a spiral path from the cell's edge to its centre. By doing so, spiral coverage addresses inefficiencies and adaptability limitations present in conventional cellular decomposition methods like Boustrophedon. Its adoption is justified by its adaptability to intricate cell geometries, confined spaces, and irregular obstructions, especially pertinent for agile applications like indoor robotics. The spiralling motion inherently leads to quicker traversal times within cells, aligning with the goal of enhancing path planning efficiency. This attribute is particularly beneficial for tasks or environments requiring rapid responses. Across a range of cell geometries—squares, circles, hexagons, and irregular polygons—the spiral coverage algorithm's versatility is underscored by tailored equations that enable

thorough exploration starting from the cell's periphery and spiralling inward, offering an encompassing approach to path planning with adaptability to various geometric properties.

3.2.1 Algorithm: spiral coverage

Start

1) Initialization:

a)Initialize the robot's position on the boundary of the given cell shape using **cellParams**.

b)Set the initial angle **θ**.

c)Set the initial spiral radius **r**.

d)Initialize the angle increment **Δθ** to control coverage density.

2)Traversal Loop:

1)While not all points in the cell are visited: Calculate the new position based on the current angle, radius, and the shape-specific equations for the given cell shape:

a)For a Square Cell:

1) $x_{new} = x_{boundary} + r \times \cos(\theta)$

2) $y_{new} = y_{boundary} + r \times \sin(\theta)$

Explanation: These equations convert polar coordinates to Cartesian coordinates, ensuring that the robot moves along the boundary and spirals inward.

b)For a Circular Cell:

1) $x_{new} = x_{center} + r \times \cos(\theta)$

2) $y_{new} = y_{center} + r \times \sin(\theta)$

Explanation: Similarly, these equations convert polar coordinates to Cartesian coordinates for circular cells.

c)For a Hexagonal Cell:

Calculate the coordinates of the hexagon's vertices and determine the robot's movement along the hexagonal boundary while spiralling inward.

1) Calculate new radius: $r_{i+1} = r_i - \Delta r$
2) Calculate new angle: $\theta_{i+1} = \theta_i + \theta_{step}$
3) Calculate new coordinates:

$x_{i+1} = x_0 + r_{i+1} * \cos(\theta_{i+1})$

$y_{i+1} = y_0 + r_{i+1} * \sin(\theta_{i+1})$

d)For an Irregular Polygonal Cell

1)Define shape-specific equations for the polygon's boundaries and adapt the robot's movement as it spirals inward.

2)Move the robot to the new position.

3)Mark the current position as visited.

4)Update the angle for the next step: **θ = θ + Δθ**.

5) If **θ** completes a full circle (2π):

6) Increment or decrement the spiral radius based on the shape-specific rules:

e) For Square and Circular Cells:

26) r = r - step_size

f) For Hexagonal and Irregular Polygonal Cells:

1) Adjust the spiral pattern to move inward or outward.

2) Adjust the angle increment and direction as needed based on the cell shape.

3) Termination:

The traversal loop terminates when all points within the cell are visited.

4)Output:

The algorithm returns the sequence of visited points, providing comprehensive coverage of the cell shape.

End

3.2.2 Explanation of terms of spiral coverage

Spiral coverage effectively navigates over irregular shapes' boundaries while spiraling inward to adapt to them. The algorithm adapts its movement patterns to each irregular shape rather than using the usual polar-to-Cartesian equations. For instance, when sweeping a garden bed with an irregular shape, the robot modifies its path to follow the outline of the bed, ensuring complete coverage without omitting any corners or confined spots. Spiral coverage provides adaptable and effective coverage in real-world circumstances with irregular borders and obstacles by adjusting its trajectory to the particular shape.

3.3 Integration of Spiral Coverage into Cellular Decomposition Algorithms

Cellular Decomposition, a fundamental technique for path planning in intricate scenarios, divides challenging regions into manageable cells. Traditional methods for the coverage of these cells with boustrophedon coverage, however, encounter limitations in time complexity. To address this, we propose the innovative concept of spiral coverage, seamlessly integrated with cellular decomposition strategies to enhance path planning. Spiral coverage adopts a systematic traversal approach, starting from the cell periphery and spiralling inwards, effectively navigating cluttered and intricate surroundings. Its ability to ensure comprehensive coverage within each cell is a notable advantage, making it particularly valuable for applications demanding full coverage such as cleaning and monitoring. Spiral Coverage excels in negotiating complex terrains, offering efficient path design by employing a methodical spiral pattern, thus addressing irregular obstacles, confined spaces, and complex geometry. Its adaptability to various cell shapes, predictability, and reproducibility further contribute to its significance. In cellular decomposition implementation, Spiral Coverage demands meticulous mathematical formulations and computational precision. The process involves defining cell parameters, translating traversal to discrete points using polar-to-Cartesian conversions, and adapting to diverse shapes through equations. Fine-tuned angle increments and dynamic spiral radii control granularity and spiralling, guided by mathematics and computer logic. This intricate algorithm, embodied through meticulous data structures, provides efficient traversal and thorough path planning within complex cell geometries, ultimately enhancing navigation efficiency.

3.3.1 ALGORITHM: Spiral Coverage Integration in Cellular Decomposition

. Initialization and Parameterization:

-Define cell shape C with geometric attributes.

- Set parameters: (x_c, y_c), R, S based on C.

2. Robot's Initial Placement:

- Initialize robot's position: (x0, y0) = (0, 0).
- Determine initial angle θ for spiral traversal.

3. Spatial Domain Partitioning:

- Partition C into discrete points P representing its boundary/vertices.

4. Angle Increment and Spiral Radius:

- Set angle increment Δθ.
- Initialize spiral radius r to maximum (boundary radius).

5. **Traversal Loop for Comprehensive Coverage:**

- Repeat until all points in P are visited:
- Calculate new position:

$x_{new} = x0 + r * \cos(\theta)$

$y_{new} = y0 + r * \sin(\theta)$

- Update position, mark point as visited, increment θ by Δθ.

6. Radius Adjustment for Inward Spiraling:

- Check if traversal completes a circle (θ increased by 2π).
- Adjust spiral radius r based on cell shape:
- For square and circular cells, decrement r by step size.
- For hexagonal and irregular polygonal cells, adapt spiral pattern.

7. Adaptation to Cell Shape:

- Ensure equations for position and radius suit specific C attributes.

8. Mathematical Formalization for Computational Implementation:

- Translate equations into code.
- Implement data structures for visited points and traversal.

9. Testing, Validation, and Optimization:

- Thoroughly test algorithm under various scenarios (obstacles).
- Validate comprehensive coverage and computational efficiency.

END

3.3.2 Explanation of the terms of Spiral Coverage Integration in cellular decomposition

The described technique describes a methodical procedure for obtaining thorough coverage inside different geometric cell forms. It starts by determining the form (C) and its geometric properties while adjusting important parameters. To start the spiral coverage, the robot's beginning position and initial traversal angle are determined. The shape is divided into distinct points along its vertices or boundaries by spatial partitioning, which affects traversal density. Polar coordinates are used by the robot to compute its new position during the traversal loop, ensuring a methodical examination of the geometry. The spiral radius is modified by the algorithm for inward spiraling, and it is modified according to the cell form to account for shape-specific complexities. Computational viability is ensured through the mathematical theory and code execution. The algorithm's effectiveness is rigorously tested, validated, and optimized in a variety of situations.

3.4 Parameters and Considerations for Optimized Spiral Coverage Integration in Rectangular Cells:

The proposed work adopts a focused approach, specifically concentrating on rectangular cell shapes, with the aim of enhancing the time efficiency of the Boustrophedon cellular breakdown methodology through the intelligent incorporation of Spiral Coverage. This section introduces the intricate parameters and multifaceted considerations necessary for the successful integration of spiral coverage in this confined context, emphasizing the pursuit of optimal path planning proficiency. Addressing the enigmatic characteristic of "Spiral Density" and achieving a delicate balance between coverage granularity and computational manageability requires meticulous calibration. The granularity of spiral traversal, governed by the angular increment denoted as θ, is selected through a careful interplay between coverage density complexities and computational finesse. Mathematical rigor and computational dexterity are employed to identify and optimize this parameter, resulting in a harmonious fusion of precision and computational efficiency tailored to rectangular cells. Another critical factor, "Spiral Radius Adjustment," dictates the algorithm's adaptability within geometric expanses of rectangular cells, involving the formulation of adjustment rules. The fine-tuning of Spiral Coverage into an efficient tool for coverage necessitates precision in parameters such as the "Initial Position and Angle" (x0, y0, θ), determining the robot's starting point and orientation on the cell's stage through a complex optimization process. In the broader context of advancing robotic applications, particularly in environmental monitoring, surveillance, and exploration, the integration of spiral coverage methodologies has emerged as a promising solution to enhance the spatial coverage capabilities of autonomous robots. This research endeavor comprehensively evaluates the performance of integrated spiral coverage methods through systematically designed experiments and rigorous evaluation criteria, contributing substantively to the field of robotics and computational geometry with a data-driven perspective on their efficacy and suitability for real-world applications.

We used the experimental design shown in Figure 5 to evaluate the Integrated Spiral Coverage Methodology's performance. Two groups were involved in this design, one utilizing the traditional approach and the other the Integrated Spiral Coverage Methodology. Test coverage,

time to coverage, and energy efficacy were among the important metrics that were measured.

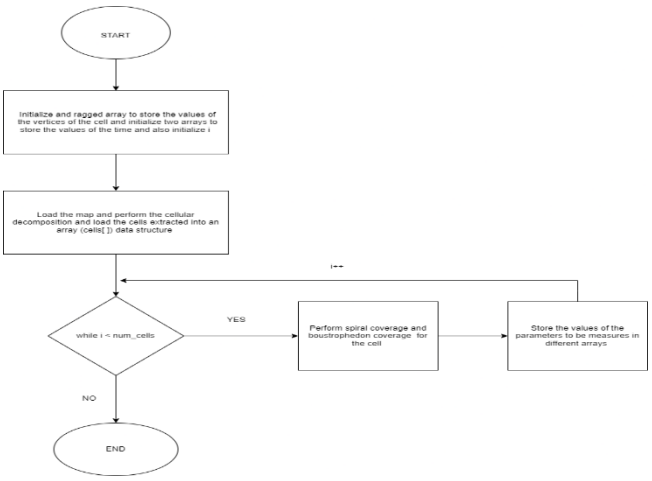

Figure 5. Experimental Design for Performance Evaluation of Integrated Spiral Coverage Methodology

3.5 Mathematical observations

In this comparative study of Boustrophedon cellular decomposition and spiral coverage for optimizing cell coverage in robotics and computational geometry, mathematical exploration was performed to unveil the intricacies of these two coverage methodologies. To analyse their performance comprehensively, we introduce a set of key variables and metrics that will allow us to draw precise comparisons and make informed observations.

Let us denote the speed of traversal in a straight line as $\mathbf{V_L}$. We will consider the number of turns taken by the spiral coverage as **Ts** and by the Boustrophedon coverage as $\mathbf{T_b}$. At each 90-degree turn, there will be a time delay denoted as $\mathbf{t_T}$. The time taken for spiral coverage will be represented as $\mathbf{t_S}$, and for Boustrophedon coverage as $\mathbf{t_B}$. We introduce the variables **R** for the number of rows, **C** for the number of columns, **Ls** for the length of the path covered in spiral coverage, and $\mathbf{L_b}$ for the length of the path covered in Boustrophedon coverage. The dimensions of each grid cell will be represented as **D x D**.

To assess the efficiency of these methodologies, we will employ a metric denoted as **E.** We examine the number of turns taken by spiral coverage, denoted as **Ns,** and by Boustrophedon coverage, denoted as **Nb**. Investigated number of waypoints in Boustrophedon coverage, designated as **kb**, and the number of waypoints in spiral coverage, represented as, **k**.

3.5.1 Consideration of three cases for the proof

- When the number of rows (R) is greater than the number of columns (C) [R > C]
- When the number of rows (R) is equal to the number of columns (C) [R = C]
- When the number of rows (R) is less than the number of columns (C) [R < C]

Analysis of three specific scenarios, each of which has yielded visual representations that encapsulate the key observations.

1) R = C [When the number of rows (R) is equal to the number of columns (C)]

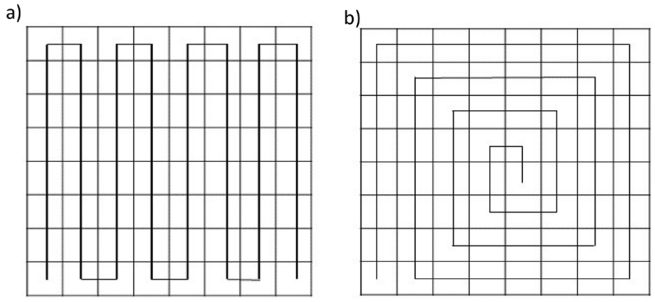

Figure 6. Represents Path planning. a) Boustrophedon cellular decomposition and b) spiral coverage for optimizing cell coverage (Number of turns = 14)

2) R > C [When the number of rows (R) is greater than the number of columns (C)]

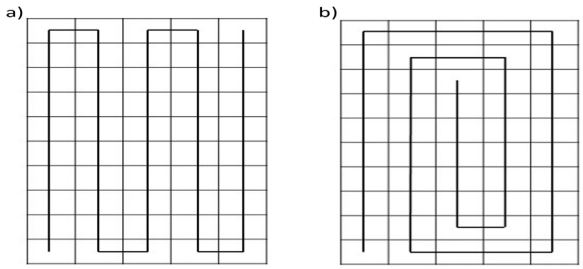

Figure 7. Represents Path planning. a) Boustrophedon cellular decomposition and b) spiral coverage for optimizing cell coverage (Number of turns = 8)

3) C > R [When the number of rows (R) is less than the number of columns (C)]

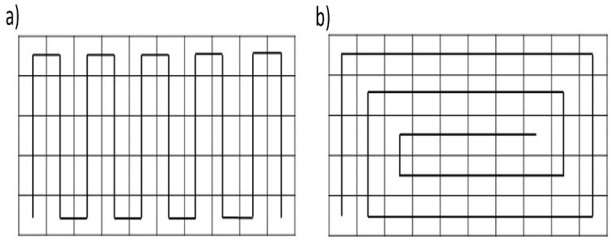

Figure 8. Represents Path planning. a) Boustrophedon cellular decomposition and b) spiral coverage for optimizing cell coverage a) Number of turns = 18 b) Number of turns= 9

Three different scenarios are taken into account while comparing Boustrophedon Coverage and Spiral Coverage, each of which shed's insight on the effectiveness of both algorithms with regard to the correlation between the number of rows (Row) and columns (Col) in grid-based coverage. The first Row > Col scenario emphasizes coverage adaptability by looking at scenarios with extended rectangular areas. The second example evaluates square regions to see how well an algorithm performs in balanced contexts. The third Col > Row scenario investigates instances of horizontally oriented rectangular areas, demonstrating flexibility in different layouts. The number of turns taken is the primary emphasis of the assessment metrics, acting as a gauge of the effectiveness of the algorithm.
From the observations made from the figure 6, 7 and 8, we conclude that the number of 90 degree turns in spiral coverage are more as compared to the boustrophedon coverage when the number of columns is greater than number of rows (C > R) and in other case those are R = C and R > C the number of turns taken by the spiral and the boustrophedon is the same. The number of turns taken by the robot in spiral and boustrophedon coverage also depend on the direction in which the robot starts covering the area. It can also be concluded from the observation that the length of the path covered by both spiral and boustrophedon always remain constant (L) this is because both spiral and boustrophedon must cover the same number grids.

Both spiral coverage and boustrophedon coverage are deterministic algorithms that traverse a grid in accordance with predetermined criteria. The robot or agent running these algorithms will ensure completeness by not skipping any grid hence this is the reason why the path length of both spiral ($\mathbf{L_s}$) and the path length of boustrophedon ($\mathbf{L_b}$) are equal.

In coverage algorithms, the degree of grid partitioning granularity has a substantial impact on coverage density. Smaller grid cells, which are indicative of finer granularity, enhance coverage density and force the robot to visit more sites for in-depth coverage, however at a cost to computation. While speeding up coverage but perhaps omitting finer details, coarse granularity, which has larger grid cells, affects coverage density. Fine granularity matches congested regions with complex obstructions, whereas coarse granularity speeds up coverage in open areas. The granularity used should be in accordance with the environment and work needs. Some systems provide dynamic granularity adjustments to optimize speed and accuracy based on real-time conditions, offering a flexible method of managing coverage density.

$$\boldsymbol{t_B} = \left(\frac{\boldsymbol{L}}{\boldsymbol{V_L}}\right) + (\boldsymbol{T_b} \times \boldsymbol{t_t}) \quad \textbf{(1)}$$

$$\boldsymbol{t_s} = \left(\frac{\boldsymbol{L}}{\boldsymbol{V_L}}\right) + (\boldsymbol{T_S} \times \boldsymbol{t_t}) \quad \textbf{(2)}$$

$$\boldsymbol{L} = \sum_{i=0}^{k} \sqrt{(\boldsymbol{x_{i+1}} - \boldsymbol{x_i})^2 + (\boldsymbol{y_{i+1}} - \boldsymbol{y_i})^2} \quad \textbf{(3)}$$

Here, k is the number of waypoints (the number of points where the robot turns in addition to the starting and ending points of its coverage). To determine the value of k for spiral and boustrophedon coverage, respectively, we can use the following formulas:

$$\boldsymbol{k_s} = (\boldsymbol{N_s} + \mathbf{2}) - \mathbf{1} \quad \textbf{(4)}$$

$$\boldsymbol{k_b} = (\boldsymbol{N_b} + \mathbf{2}) - \mathbf{1} \quad \textbf{(5)}$$

According to these findings, the boustrophedon motion makes more 90-degree turns than the spiral motion does when C > R, and in the circumstances where R = C and R > C, the number of turns made is constant. The path length is also constant for both spiral and boustrophedon coverage. Combining these findings with equations (1) and (2), it is evident that spiral motion will cover the specified area faster than boustrophedon motion.
Now let us study the turning in spiral and boustrophedon motion. **Figure 9** depicts the turning motion in boustrophedon motion and the spiral motion using grid which shows spiral motion takes one 90-degree turns whereas boustrophedon motion takes only one 90-degree turn.

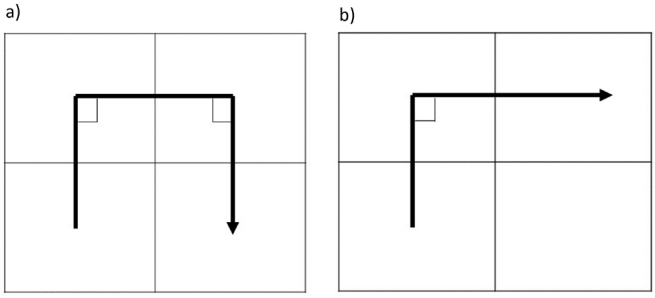

Figure 9. Depiction of the turning motion using grid. a) Boustrophedon motion, b) the spiral motion.

A robot's ability to make a 90-degree turn is influenced by various factors, including control and mechanical issues. Turning involves a complex process of deceleration, rotation, and acceleration, leading to potential time and energy consumption. Mechanical constraints, especially in wheel-equipped robots, can further limit turning speed or impose minimum turning radii. Sensor adjustments during turns introduce additional delays, impacting navigation and obstacle avoidance. Safety concerns may lead to intentional slowing down during turns to maintain stability, prolonging the turning process. Control algorithms designed for smooth motion may contribute to gradual transitions during turns, extending the required time. The robot's kinematics and inertia, influenced by size, mass, and wheel arrangement, also affect turning capabilities. Figure 9 graphically depicts two turning patterns: a) Boustrophedon motion and b) spiral motion, offering insights into the complexities of turning within a grid setting and aiding in visualizing different motion characteristics.

For calculating the efficiency metrics, the formula derived is as follows:

$$\boldsymbol{E} = \frac{\boldsymbol{t_s}}{\boldsymbol{t_b}} \qquad (6)$$

Here **E** is the efficiency of the spiral coverage as compared to the boustrophedon coverage.

From equation (1), (2) and (6) we get,

$$\boldsymbol{E} = \frac{\boldsymbol{T_s}}{\boldsymbol{T_b}} \qquad (7)$$

Formula 6 and 7 are two formulas that can be used to measure how well Spiral Coverage outperforms Boustrophedon Coverage. E, which is computed as the ratio of the time required for Spiral Coverage (t_s) to that required for Boustrophedon Coverage (t_b), stands for the efficiency of Spiral Coverage relative to Boustrophedon Coverage in the first equation. This ratio indicates how much Spiral Coverage outperforms its grid-based counterpart in finishing a certain assignment. The second equation expands this comparison to include the overall work duration. The efficiency factor, still known as E in this instance, is now the ratio of the total time for spiral coverage (T_s) to the total time for boustrophedon coverage (T_b).

1.5 Dynamic Power-Consumption .

$$E = \int (P(t) \times dt) \qquad (8)$$

In equation 8 the complex interaction between the time dimension and the energy aspects in the context of robotic systems can be summarized by the general formula E = ∫(P(t) × dt), in which E is the total energy expended throughout the performance of a complex job. The variable P(t) represents the power that the robot's various parts and modules draw over time, which dynamically shapes the energy consumption. The way this is expressed emphasizes the complex relationships between energy consumption and the power dynamics' temporal evolution. This means that evaluating, tracking, and optimizing the robot's energy profile in the diverse and constantly shifting domain of real-world tasks requires a comprehensive approach

4. Results and Discussion

This study concentrates on rectangular obstacles, specifically exploring how the Spiral Coverage algorithm reduces coverage time within rectangular cells resulting from area cellular decomposition. Three environments with varying obstacle density and size were considered: the first (Fig. 12) with three obstacles, the second (Fig. 13) with four obstacles, and the third (Fig. 14) with five obstacles. No specific considerations were made regarding obstacle size. Implementation of the Spiral Coverage algorithm in Python, coupled with a custom Pygame simulator, facilitated experimentation across diverse environments with rectangular obstacles. The simulation visually and quantitatively assessed Spiral Coverage performance in different scenarios. A Pygame-based graphical representation depicted two grid traversal algorithms—lawnmower and spiral traversal. The simulation incorporated parameters like grid size, cell size, delay, and color, with a stopwatch measuring traversal time. The size of the grid and the number of rows and columns influenced the radius of spiral coverage, balancing even spacing and aesthetic preferences. Empirical findings on rectangular cell coverage efficiency compared Spiral Coverage with traditional Boustrophedon methods

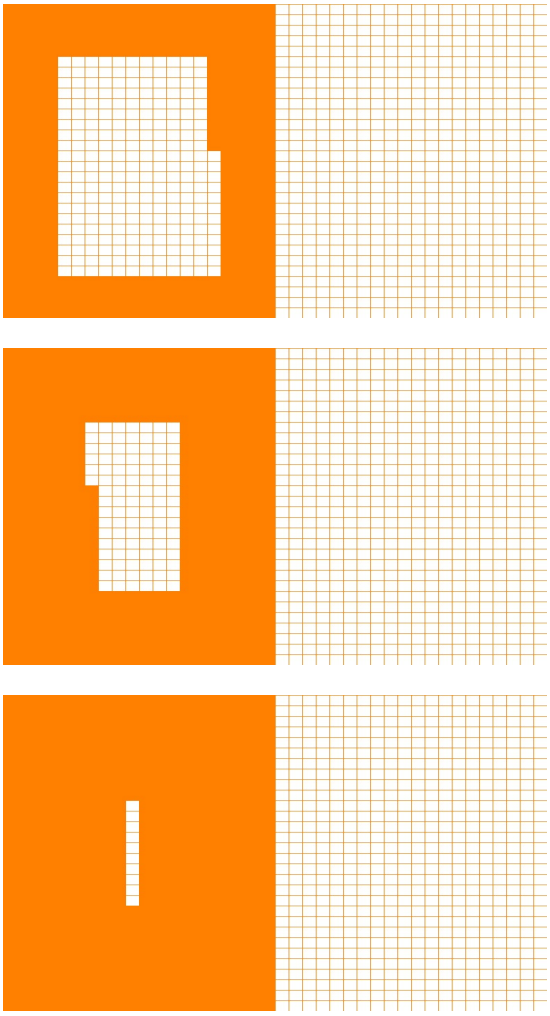

Figure 10. shows the different stages of the spiral coverage in the pygame simulator that we have built for this experiment.

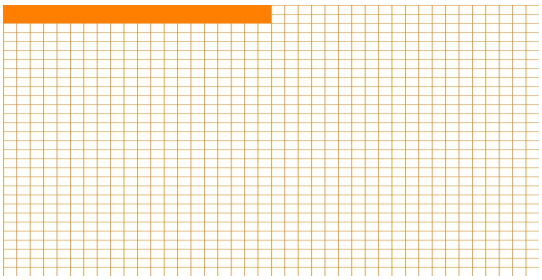

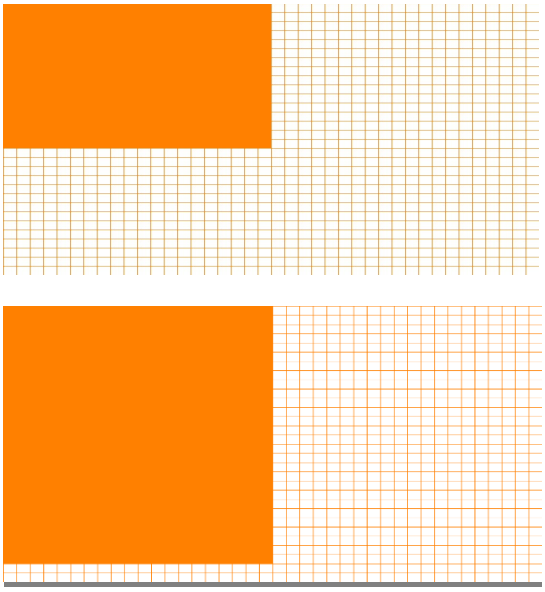

Figure 11. shows the different stages of the boustrophedon coverage in the pygame simulator for which we have built for these algorithm.

Figures 10 and 11 show different coverage phases using the Boustrophedon and Spiral approaches in the context of our Pygame simulator. These graphics depict several stages of the simulation and provide information about the dynamic evolution and unique features of the Boustrophedon and Spiral coverage methods. These graphics offer a concrete look at the changing geographical coverage patterns that the Pygame environment simulates.

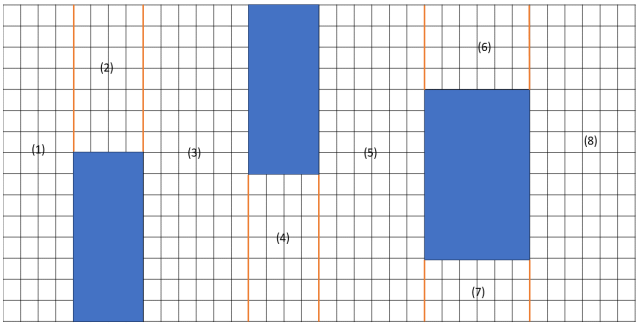

Figure 12. Depiction of different environments used for the experimental analysis. Dimensions of each cell – this is in the format of (rows x columns) (1) 9 x 4 (2) 16 x 3 (3) 8 x 6 (4) 16 x 5 (5) 8 x 14 (6) 2 x 14

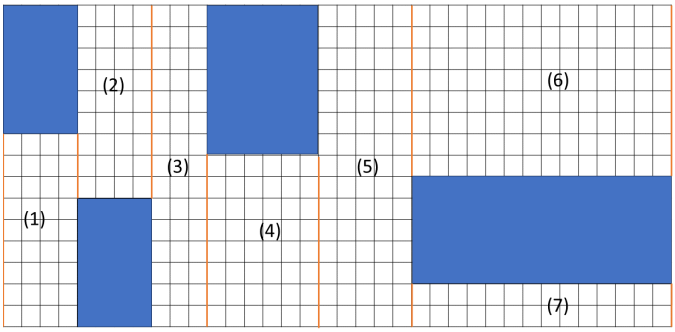

Figure 13. Depiction of dimensions of each cell (rows x columns) (1)16 x 4 (2) 7 x 4 (3) 16 x 6 (4) 7 x 4 (5) 16 x 6 (6) 4 x 6 (7) 3 x 6 (8)16 x 6

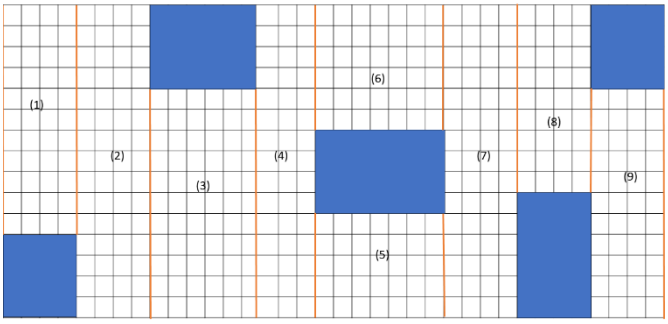

Figure 14. Depiction of dimensions of each cell (rows x columns) (1) 11 x 4 (2) 16 x 4 (3) 12 x 6 (4) 16 x 3 (5) 5 x 7 (6) 6 x 7 (7) 16 x 4 (8) 10 x 4 (9) 12 x 4

The three diagrams shown in figure 12, 13 and 14 show various levels of obstacle density in a setting. Three distributed rectangular obstacles are the only obstacles in the first diagram's sparsely populated environment. The terrain is broken into smaller cells to allow for more precise robot navigation within each cell that is free of obstacles. The second diagram uses cells to balance coverage effectiveness and obstacle avoidance in a moderately congested area with a denser distribution of obstacles. The third diagram shows a very congested landscape with close-knit rectangular obstructions. In this situation, a cell decomposition method is used to ease robot mobility inside the heavily obstructed environment and ensure efficient traversal within each cell free of obstacles.

The experimental environments shown in the figures 12, 13 and 14 were designed to feature varying obstacle densities. After conducting cellular decomposition, the dimensions of resulting rectangular cells were measured. These rectangular cells were subjected to testing within the simulator to gauge the time needed for their coverage, and this time was compared to the coverage times achieved by both the spiral coverage and Boustrophedon coverage methods.

Let $\mathbf{t_b}$ be the time required to cover the area through boustrophedon coverage and $\mathbf{t_s}$ be the time required to cover the area through spiral coverage.

Table 1. Time required to cover each cell by boustrophedon coverage and the spiral coverage

Cell number	Size of the cell (r x c)	Time for boustrophedon Coverage(seconds)	Time for spiral Coverage(seconds)
(1)	9 x 4	4	2
(2)	9 x 4	4	2
(3)	16 x 3	8	1
(4)	8 x 6	4	3
(5)	16 x 5	8	3
(6)	8 x 14	5	4
(7)	2 x 14	1	1

As can be seen table 1 represents the time required to cover each cell in the by boustrophedon coverage and the spiral coverage respectively in figure 12. For the region in figure 12 $\mathbf{t_b}$ = 34 seconds and $\mathbf{t_s}$ = 16 seconds

Table 2. Time required to cover each cell by boustrophedon coverage and the spiral coverage.

Cell number	Size of the cell (r x c)	Time for boustrophedon Coverage(seconds)	Time for spiral Coverage(seconds)
(1)	16x 4	8	2
(2)	7 x 4	3	2
(3)	16 x 6	8	3
(4)	7 x 4	3	2
(5)	16 x 6	8	3
(6)	4 x 6	2	2
(7)	3 x 6	1	1
(8)	16 x 6	8	3

According to Figure 13. Results can be depicted in table 2 representing the time required to cover each cell by boustrophedon coverage and the spiral coverage respectively. For the region in figure 13, $\mathbf{t_b}$ = 41 seconds and $\mathbf{t_s}$ = 18 seconds.

Table 3. Time required to cover each cell by boustrophedon coverage and the spiral coverage

Cell number	Size of the cell (r x c)	Time for boustrophedon Coverage(seconds)	Time for spiral Coverage(seconds)
(1)	11 x 4	2	5
(2)	16 x 4	8	2
(3)	12 x 6	6	3
(4)	16 x 3	8	1
(5)	5 x 7	2	2
(6)	6 x 7	3	3
(7)	16 x 4	8	2
(8)	10 x 4	5	2
(9)	12 x 4	6	2

According to figure 14, results can be tabulated as shown in table 3, representing the time required to cover each cell in the by boustrophedon coverage and the spiral coverage respectively. For the region in figure 14, $\mathbf{t_b}$ = 48 seconds and $\mathbf{t_s}$ = 22 seconds

Both spiral and boustrophedon (lawnmower) coverage of n cells have linear computing complexity, defined as O(n). The number of cells visited grows linearly with the total number of cells in the spiral coverage, where cells are visited in a spiral pattern, and in the boustrophedon coverage, where cells are covered row by row, leading to effective algorithms with linear time complexity. Due to their linear computational complexity, both approaches are suited for grid-based traversal jobs as the time required for traversal will scale linearly with the number of cells to be covered.

Both spiral and boustrophedon (lawnmower) coverage of n cells have linear computing complexity, defined as O(n). The number of cells visited grows linearly with the total number of cells in the spiral coverage, where cells are visited in a spiral pattern, and in the boustrophedon coverage, where cells are covered row by row, leading to effective algorithms with linear time complexity. Due to their linear computational complexity, both approaches are suited for grid-based traversal jobs as the time required for

traversal will scale linearly with the number of cells to be covered.

Table 4 . efficiency of the spiral coverage w.r.t the boustrophedon coverage according to formula 6

Table no	Efficiency of spiral w.r.t boustrophedon coverage
1	0.47
2	0.43
3	0.45
	Average = 0.45

The comparative analysis between the time taken be boustrophedon coverage and the spiral coverage within each cell in each of the region is tabulated in the **Figure 15.**

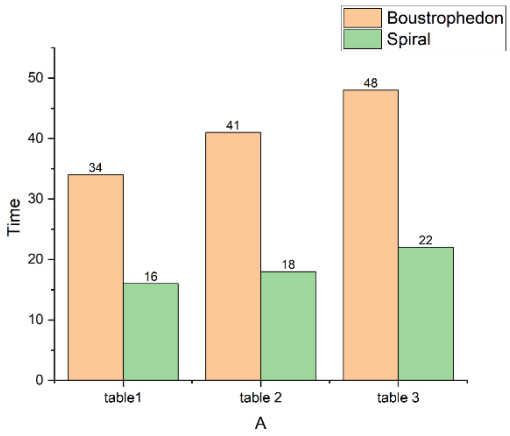

Figure 15. The Comparative Analysis Between the Time Taken Be Boustrophedon Coverage and The Spiral Coverage applied in table 1, table 2 and table 3

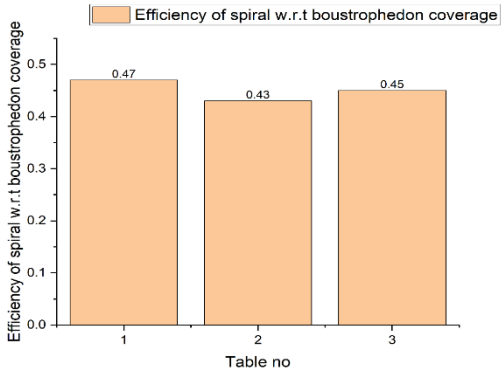

Figure 16. this figure shows the efficiency of the spiral coverage w.r.t boustrophedon coverage applied in table 1, table 2 and table 3.

The comparison results shown in Tables 1, 2, and 3 offer a thorough evaluation of the temporal effectiveness as plotted in Figure 16 of both Boustrophedon and Spiral coverage strategies across various obstacle densities, offering insightful information about their practical usefulness. The Spiral coverage regularly outperforms the Boustrophedon coverage in the cases shown in Figure 12, 13 and 14 taking a lot less time to cover each cell. This pattern is continued in Figure 14, where the performance of both techniques is true when the grid size and cell size are changed. from table 4 we can conclude that the spiral coverage has an a average efficiency of 0.45 which implies that spiral coverage is 45% better than the boustrophedon coverage for cellular decomposition.

While our algorithm focuses on rectangular obstacles to enhance efficiency, it's essential to acknowledge the limitation of not accounting for more diverse and irregular obstacle shapes present in real-world scenarios. Extending our strategy to encompass a broader range of obstacle shapes could enhance adaptability and applicability. Comparatively, Young-Ho Choi et al.'s Linking Spiral Paths through a Constrained Inverse Distance Transform (LSP-CIDT) [28] achieves approximately 91% efficiency in area coverage, yet the algorithm exhibits a high number of turns, lacking assessment for time efficiency. In our study, we tested Spiral Coverage against Boustrophedon coverage, revealing a 45% improvement on average in favour of Spiral Coverage. Similarly, the Energy-aware Spiral Coverage Path Planning algorithm [29] offers a time and energy comparison with Boustrophedon coverage but indicates a 9%-time reduction for E-Spiral. In contrast, our results demonstrate a 45% efficiency gain for Spiral Coverage within each cell, surpassing the proposed E-Spiral algorithm. In robot simulation, considering power and energy properties is crucial for accurate modelling, allowing researchers to mimic realistic robot behaviours and assess performance under various conditions, ensuring simulations align with real-world restrictions
In this case we have fixed the power of the robot to 1 and we are assuming that while starting the coverage of each of the environment the robot is fully charged

Table 5 . shows the energy efficiency of the spiral and boustrophedon coverage in figure 12 , 13 and 14 with the help of formula 8

Table no.	Energy consumed by boustrophedon coverage (E_b) (joule (J))	Energy consumed by spiral coverage (E_s) (joule (J))
1	1* 34 = 34	16
2	1 * 41 = 41	18
3	1 * 48 = 48	22

The energy consumption of the Boustrophedon and Spiral coverage path planning techniques across several situations is shown in a simple and straightforward manner in table 5. Interestingly, Spiral covering constantly performs better than Boustrophedon Coverage, using a substantially

smaller amount of energy (measured in joules) to finish the covering objective. This demonstrates how effective Spiral Coverage is as an energy-efficient method of path design in a variety of settings. Table 5 has been visually depicted in figure 17 which shows how spiral coverage consumes less energy for coverage as compared to boustrophedon coverage.

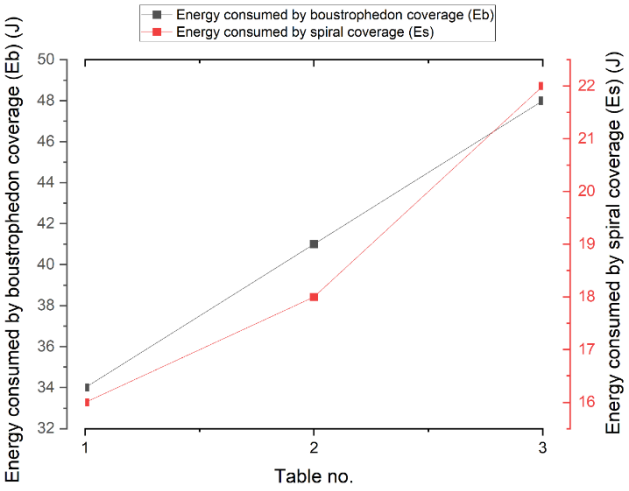

Figure 17. shows the comparative graph between the energy consumed by the spiral cover age and boustrophedon coverage in figure 11 , 12 and 13.

On average, spiral coverage demonstrates a 45% improvement over existing boustrophedon coverage in robotic path planning. The systematic inward motion of the spiral pattern proves advantageous for thorough coverage of rectangular surfaces, minimizing the risk of overlooking areas within the rectangle. Particularly beneficial for tasks requiring focused concentration or a specific completion point in a rectangular space, the spiral pattern ensures methodical and efficient coverage from the periphery to the center. However, drawbacks include potential inefficiencies and higher energy usage due to increased path overlap. The systematic inward motion may also complicate adaptation to obstructions and irregular shapes within the rectangle, impacting coverage efficiency in confined spaces. Additionally, challenges in adjusting to different rectangular space sizes and potential backtracking issues should be carefully considered, weighing the benefits against the drawbacks in alignment with task and environmental requirements.

5. Conclusion

In this study, we aimed to enhance path planning efficiency by incorporating the Spiral Coverage algorithm into a framework based on rectangular cell traversal. Using Python programming and a custom Pygame simulator, experiments were conducted in diverse environments containing rectangular obstacles, providing valuable insights into the algorithm's behavior under varying conditions. Comparative analysis with Boustrophedon coverage revealed that Spiral Coverage consistently outperformed in terms of time efficiency across different cell sizes and obstacle densities. The results indicated notable time savings, with Spiral Coverage completing tasks significantly faster than Boustrophedon coverage in various cases. For instance, Spiral Coverage averaged 16 seconds compared to Boustrophedon coverage's 34 seconds in one scenario, demonstrating its effectiveness in diverse path planning applications, particularly in environments with rectangular obstacles. The integration of Spiral Coverage holds practical significance for fields like robotics and automation, where efficient path planning is crucial. The future directions in this field are promising, with a trajectory towards advanced autonomy and efficiency for robotic systems. The incorporation of hybrid path planning strategies, merging Spiral Coverage with Boustrophedon methods, stands out as a significant leap in autonomous robotics. These hybrid algorithms offer enhanced adaptability in challenging terrains and dynamic environments, further amplified by cutting-edge sensor technologies such as computer vision and LiDAR [30]. The ongoing evolution of research will emphasize coordinated multi-robot systems, optimizing energy consumption without compromising coverage quality through sophisticated algorithms [32]. Rigorous testing in diverse real-world settings will validate theoretical advancements and contribute to the practical implementation of these strategies [33]. Responsible deployment will be guided by standardization initiatives, ethical considerations, and safety procedures [34, 35]. With a focus on human-centric applications like healthcare, environmental monitoring, and search and rescue, the future landscape of robotics holds the promise of unprecedented efficiency and versatility. This paper lays the groundwork for upcoming research, particularly in refining algorithms to significantly reduce traversal time for different shapes and enhancing the overall time complexity of coverage path planning strategies.

References

[1] De Carvalho RN, Vidal HA, Vieira P, Ribeiro MI. Complete coverage path planning and guidance for cleaning robots. InISIE'97 Proceeding of the IEEE International Symposium on Industrial Electronics 1997 Jul 7 (Vol. 2, pp. 677-682). IEEE.

[2] Huang Y, Cao Z, Hall E. Region filling operations for mobile robot using computer graphics. InProceedings. 1986 IEEE International Conference on Robotics and Automation 1986 Apr 7 (Vol. 3, pp. 1607-1614). IEEE.

[3] Hameed IA. Motion planning for autonomous landmine detection and clearance robots. In2016 International Workshop on Recent Advances in Robotics and Sensor Technology for Humanitarian Demining and Counter-IEDs (RST) 2016 Oct 27 (pp. 1-5). IEEE.

[4] Ollis M, Stentz A. First results in vision-based crop line tracking. InProceedings of IEEE International Conference on Robotics and Automation 1996 Apr 22 (Vol. 1, pp. 951-956). IEEE.
[5] Brooks R. A robust layered control system for a mobile robot. IEEE journal on robotics and automation. 1986 Mar;2(1):14-23.
[6] Gage DW. Randomized search strategies with imperfect sensors. InMobile Robots VIII 1994 Feb 1 (Vol. 2058, pp. 270-279). SPIE.
[7] Galceran E, Carreras M. A survey on coverage path planning for robotics. Robotics and Autonomous systems. 2013 Dec 1;61(12):1258-76.
[8] Choset H. Coverage of known spaces: The boustrophedon cellular decomposition. Autonomous Robots. 2000 Dec;9:247-53.
[9] Gao L, Lv W, Yan X, Han Y. Complete coverage path planning algorithm based on energy compensation and obstacle vectorization. Expert Systems with Applications. 2022 Oct 1;203:117495.
[10] Song J, Gupta S. $\varepsilon^{\star} $: An Online Coverage Path Planning Algorithm. IEEE Transactions on Robotics. 2018 Feb 8;34(2):526-33.
[11] Bochkarev S, Smith SL. On minimizing turns in robot coverage path planning. In2016 IEEE international conference on automation science and engineering (CASE) 2016 Aug 21 (pp. 1237-1242). IEEE.
[12] Choset H. Coverage of known spaces: The boustrophedon cellular decomposition. Autonomous Robots. 2000 Dec;9:247-53.
[13] Ntawumenyikizaba A, Viet HH, Chung T. An online complete coverage algorithm for cleaning robots based on boustrophedon motions and A* search. In2012 8th International Conference on Information Science and Digital Content Technology (ICIDT2012) 2012 Jun 26 (Vol. 2, pp. 401-405). IEEE.
[14] Hassan M, Liu D, Chen X. Squircular-CPP: A smooth coverage path planning algorithm based on squircular fitting and spiral path. In2020 IEEE/ASME International Conference on Advanced Intelligent Mechatronics (AIM) 2020 Jul 6 (pp. 1075-1081). IEEE.
[15] Van Pham H, Asadi F, Abut N, Kandilli I. Hybrid spiral STC-hedge algebras model in knowledge reasonings for robot coverage path planning and its applications. Applied Sciences. 2019 May 9;9(9):1909.
[16] Fevgas G, Lagkas T, Argyriou V, Sarigiannidis P. Coverage path planning methods focusing on energy efficient and cooperative strategies for unmanned aerial vehicles. Sensors. 2022 Feb 6;22(3):1235.
[17] Khan A, Noreen I, Habib Z. On Complete Coverage Path Planning Algorithms for Non-holonomic Mobile Robots: Survey and Challenges. J. Inf. Sci. Eng.. 2017 Jan 1;33(1):101-21.
[18] Heydari J, Saha O, Ganapathy V. Reinforcement learning-based coverage path planning with implicit cellular decomposition. arXiv preprint arXiv:2110.09018. 2021 Oct 18.
[19] Jensen-Nau KR, Hermans T, Leang KK. Near-optimal area-coverage path planning of energy-constrained aerial robots with application in autonomous environmental monitoring. IEEE Transactions on Automation Science and Engineering. 2020 Aug 31;18(3):1453-68.
[20] Kumar K, Kumar N. Region coverage-aware path planning for unmanned aerial vehicles: A systematic review. Physical Communication. 2023 Apr 18:102073.
[21] Balampanis F, Maza I, Ollero A. Area partition for coastal regions with multiple UAS. Journal of Intelligent & Robotic Systems. 2017 Dec;88:751-66.
[22] Brown S, Waslander SL. The constriction decomposition method for coverage path planning. In2016 IEEE/RSJ International Conference on Intelligent Robots and Systems (IROS) 2016 Oct 9 (pp. 3233-3238). IEEE.
[23] Lin HY, Huang YC. Collaborative complete coverage and path planning for multi-robot exploration. Sensors. 2021 May 26;21(11):3709.
[24] Balampanis F, Maza I, Ollero A. Area decomposition, partition and coverage with multiple remotely piloted aircraft systems operating in coastal regions. In2016 International Conference on Unmanned Aircraft Systems (ICUAS) 2016 Jun 7 (pp. 275-283). IEEE.
[25] Wu C, Dai C, Gong X, Liu YJ, Wang J, Gu XD, Wang CC. Energy-efficient coverage path planning for general terrain surfaces. IEEE Robotics and Automation Letters. 2019 Feb 17;4(3):2584-91.
[26] Yang T, Miro JV, Lai Q, Wang Y, Xiong R. Cellular decomposition for nonrepetitive coverage task with minimum discontinuities. IEEE/ASME Transactions on Mechatronics. 2020 May 5;25(4):1698-708.
[27] Barrientos A, Colorado J, Cerro JD, Martinez A, Rossi C, Sanz D, Valente J. Aerial remote sensing in agriculture: A practical approach to area coverage and path planning for fleets of mini aerial robots. Journal of Field Robotics. 2011 Sep;28(5):667-89.
[28] Choi, Y.H., Lee, T.K., Baek, S.H. and Oh, S.Y., 2009, October. Online complete coverage path planning for mobile robots based on linked spiral paths using constrained inverse distance transform. In 2009 IEEE/RSJ International Conference on Intelligent Robots and Systems (pp. 5788-5793). IEEE.
[29] Cabreira TM, Di Franco C, Ferreira PR, Buttazzo GC. Energy-aware spiral coverage path planning for uav photogrammetric applications. IEEE Robotics and automation letters. 2018 Jul 16;3(4):3662-8.
[30] Alfred Daniel J, Chandru Vignesh C, Muthu BA, Senthil Kumar R, Sivaparthipan CB, Marin CE. Fully convolutional neural networks for LIDAR–camera fusion for pedestrian detection in autonomous vehicle. Multimedia Tools and Applications. 2023 Feb 1:1-24.
[31] Saadallah A, Finkeldey F, Buß J, Morik K, Wiederkehr P, Rhode W. Simulation and sensor data fusion for machine learning application. Advanced Engineering Informatics. 2022 Apr 1;52:101600.
[32] Velhal S, Sundaram S, Sundararajan N. A decentralized multirobot spatiotemporal multitask assignment approach for perimeter defense. IEEE Transactions on Robotics. 2022 Mar 28;38(5):3085-96.
[33] Krell E, King SA, Carrillo LR. Autonomous Surface Vehicle energy-efficient and reward-based path planning using Particle Swarm Optimization and Visibility Graphs. Applied Ocean Research. 2022 May 1;122:103125.
[34] Benos L, Sørensen CG, Bochtis D. Field deployment of robotic Systems for Agriculture in light of key safety, labor, ethics and legislation issues. Current Robotics Reports. 2022 Jun;3(2):49-56.
[35] Mezgár I, Váncza J. From ethics to standards–A path via responsible AI to cyber-physical production systems. Annual Reviews in Control. 2022 Jan 1;53:391-404.